



HAL
open science

Bacterial characterization in ambient submicron particles during severe haze episodes at Ji'nan, China

Caihong Xu, Min Wei, Jianmin Chen, Xinfeng Wang, Chao Zhu, Jiarong Li, Lulu Zheng, Guodong Sui, Weijun Li, Wenxing Wang, et al.

► To cite this version:

Caihong Xu, Min Wei, Jianmin Chen, Xinfeng Wang, Chao Zhu, et al.. Bacterial characterization in ambient submicron particles during severe haze episodes at Ji'nan, China. *Science of the Total Environment*, 2017, 580, pp.188-196. 10.1016/j.scitotenv.2016.11.145 . hal-01741196

HAL Id: hal-01741196

<https://hal.science/hal-01741196>

Submitted on 22 Mar 2018

HAL is a multi-disciplinary open access archive for the deposit and dissemination of scientific research documents, whether they are published or not. The documents may come from teaching and research institutions in France or abroad, or from public or private research centers.

L'archive ouverte pluridisciplinaire **HAL**, est destinée au dépôt et à la diffusion de documents scientifiques de niveau recherche, publiés ou non, émanant des établissements d'enseignement et de recherche français ou étrangers, des laboratoires publics ou privés.

1 **Bacterial Characterization in Ambient Submicron Particles during**
2 **Severe Haze Episodes at Ji'nan, China**

3 Caihong Xu[†], Min Wei[†], Jianmin Chen^{†,‡,*}, Xinfeng Wang[†], Chao Zhu[†], Jiarong Li[†], Lulu
4 Zheng[‡], Guodong Sui[‡], Weijun Li[†], Wenxing Wang[†], Qingzhu Zhang[†], Abdelwahid
5 Mellouki^{†,§}

6 [†] Environment Research Institute, School of Environmental Science and Engineering,
7 Shandong University, Ji'nan 250100, China

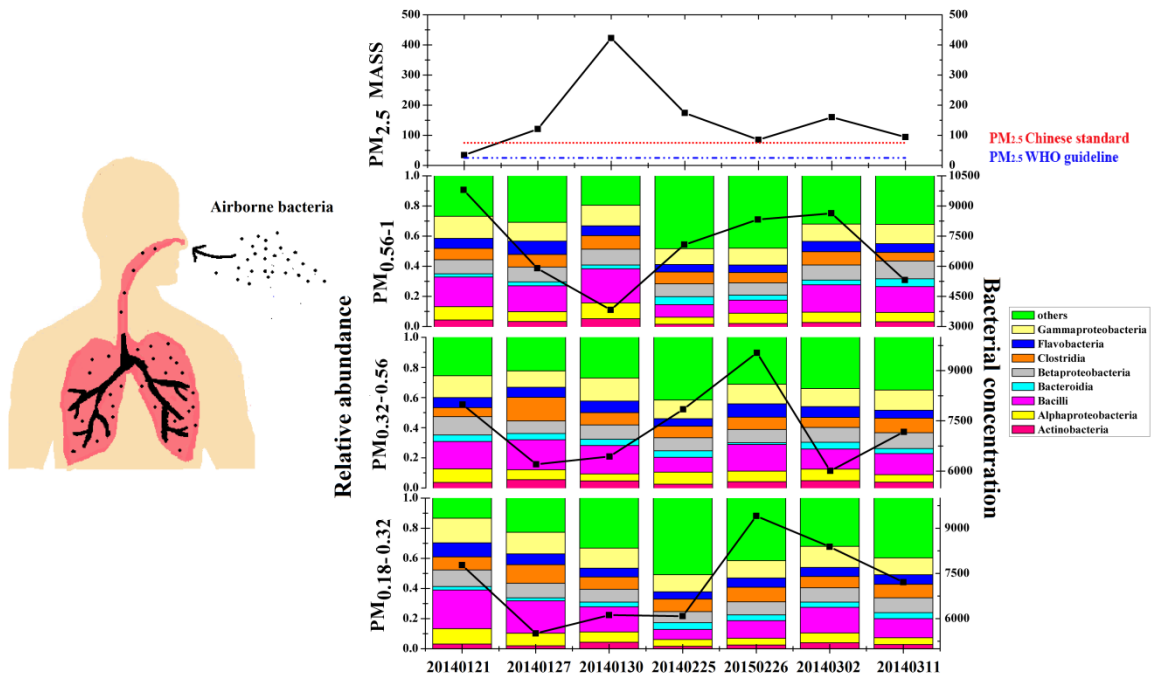
8 [‡] Shanghai Key Laboratory of Atmospheric Particle Pollution and Prevention (LAP), Fudan
9 Tyndall Centre, Department of Environmental Science & Engineering, Fudan University,
10 Shanghai 200433, China

11 [§] Institut de Combustion, Aérothermique, Réactivité et Environnement, CNRS, 45071
12 Orléans cedex 02, France

13 * Corresponding author

14 *E-mail* address: jmchen@sdu.edu.cn or jmchen@fudan.edu.cn. (J. M. Chen)

15 **Graphic Abstract**



16

17 **HIGHLIGHTS**

- 18 1. High bacterial concentration and diverse bacterial community in submicron particles
 19 (PM_{0.18-0.32}, PM_{0.32-0.56}, and PM_{0.56-1}) during haze episodes were observed.
 20 2. The bacterial community varied significantly via different size fractions.
 21 3. Source track analysis showed that the ambient bacteria mainly originated from soils, leaf
 22 surfaces, and feces.

23 **ABSTRACT**

24 In January 2014, severe haze episodes which sweep across Chinese cities have attracted
25 public concern and interest at home and abroad. In addition to the physicochemical properties
26 of air pollutants, bacteria are thought to be responsible for the spread of respiratory diseases
27 and various allergies. We attempted the bacterial characterization of submicron particles
28 (PM_{0.18-0.32}, PM_{0.32-0.56}, and PM_{0.56-1}) under severe haze episodes using high-throughput
29 sequencing and real-time quantitative PCR detecting system based on 21 samples collected
30 from January to March 2014 at Ji'nan, China. The high bacterial concentration in PM_{0.32-0.56}
31 (7314 cells·m⁻³), PM_{0.18-0.3} (7212 cells·m⁻³), and PM_{0.56-1} (6982 cells·m⁻³) showed significant
32 negative correlations with SO₂, NO₂, and O₃. Under sufficient sequencing depth, 37 phyla,
33 71 classes, 137 orders, 236 families, and 378 genera were classified, and the bacterial
34 community structure varied significantly in different size fractions. For example,
35 Holophagaceae (Acidobacteria) in PM_{0.32-0.56} showed 6-fold higher abundance than that in
36 PM_{0.18-0.32}. Moreover, functional categories and bacterial species (*Lactococcus piscium*,
37 *Pseudomonas fragi*, *Streptococcus agalactiae*, and *Pseudomonas cichorii*) that may
38 potentially be responsible for infections and allergies were also discovered. Source track
39 analysis showed that the ambient bacteria mainly originated from soils, leaf surfaces, and
40 feces. Our results highlighted the importance of airborne microbial communities by
41 understanding the concentration, structure, ecological and health effects, especially those in
42 submicron particles during haze episodes.

43 **Keywords:** Bioaerosol; Haze; Bacterial community; Submicron particles

44 1. Introduction

45 In the last few decades, the rapid economic growth and energy consumption, along with the
46 lack of measures for protecting atmospheric environments, has resulted in continuous haze
47 episodes in China (Yang et al., 2015; Li et al., 2014). In severe haze episodes, the daily
48 average PM_{2.5} mass concentration of Jing-Jin-Ji regions (Wang et al., 2013; Han et al., 2016)
49 largely exceeded 25 $\mu\text{g}\cdot\text{m}^{-3}$, which is specified as the limit of the World Health
50 Organization(WHO) PM_{2.5} health guideline, by about 20-fold. Exposure to such high
51 concentrations of airborne particles leads to high morbidity and mortality due to infectious
52 diseases such as cardiovascular diseases, respiratory infections, and lung cancer (Bower et
53 al., 2013; Esposito et al., 2012). Based on the definition of haze by the State Standard of the
54 People's Republic of China (QX/T 113-2010), haze is defined as a complex air pollution
55 process include the following conditions: (1) visibility less than 10 km and relative humidity
56 lower than 80%, and (2) the PM_{2.5} mass concentration higher than 75 $\mu\text{g}\cdot\text{m}^{-3}$ (Leng et al.,
57 2013; Kong et al., 2014; Jansen et al., 2014; China Meteorological Administration, 2010). In
58 January of 2013 and 2014, severe haze episodes were reported in Beijing (Wei et al., 2016),
59 Hebei (Wang et al., 2013), Nanjing (Kong et al., 2015), and Ji'nan (Wang et al., 2015a) which
60 caused great economic losses and public panic across China. Ji'nan is the capital of Shandong
61 Province and covers an area of 8177 km². It is surrounded by hills on three sides which may
62 exacerbate the accumulation of airborne pollutants including atmospheric particles, sulfur
63 dioxide, nitrogen oxide, trace gases, and volatile organic compounds (Liu et al., 2015; Zhang
64 et al., 2014; Li et al., 2011). Majority of existing studies focussed on the bacteria which
65 occupied about 80.8% and 86.1% of the total microbes (Cao et al., 2014) in PM_{2.5} and PM₁₀.
66 Limited studies investigated bacteria in submicron particles (Gou et al. 2016), which can
67 easily penetrate lungs or even the blood stream (Janssen et al., 2011; Visser et al., 2015; Gao
68 et al., 2015b). Hence it is essential to study the bacterial characteristics of such

69 aforementioned submicron particles in atmosphere.

70 The near-surface and upper troposphere contain thousands to millions of bacterial cells per
71 cubic meter (Bower et al. 2012). Active bacteria can serve as a medium for the spread of
72 allergens and pathogens in a crowd (Creamean et al., 2013; Husman et al., 1996). There are
73 also increasing evidences indicating that bacteria can act as cloud condensation nuclei,
74 absorbing or reflecting sunlight, or even participating in N-cycling and C-cycling in the
75 ecosystem (Bauer et al., 2003). So far, many investigations on the active bacterial
76 concentration and bacterial community in airborne particles have been conducted (Bertolini
77 et al., 2013; Hospodsky et al., 2015; Prussin et al., 2015). The airborne bacterial concentration
78 in the near-surface ranged from 10^4 to 10^6 cells·m⁻³ (Bowers et al., 2012; Haas et al., 2013;
79 Murata et al., 2014; Goudarzi et al. 2014; Murata et al., 2016). Bower et al. (2013) reported
80 detailed information on the airborne microbial community and sources in PM_{2.5} and PM_{2.5-10}
81 and found that the bacterial richness and communities structures showed a significant
82 distinction across these two size fractions. In China, Cao et al. (2014) described the microbial
83 communities of PM_{2.5} and PM₁₀ using metagenomics during a serious smog event and found
84 that bacteria were the dominant one which was mostly terrestrial-related. Wei et al. (2016)
85 investigated the concentration and size distribution of bioaerosols during haze and sunny
86 days in Beijing. Compared to the sunny day, the fluorescent particle concentrations increased
87 during the haze episodes and decreased with the dissipation of haze occurrences in 3-5 days.
88 Furthermore no obvious difference in the airborne bacterial abundance and community
89 structure were observed between haze and sunny days. Although these studies have
90 illustrated the concentration and community compositions of cultured or uncultured bacteria
91 in atmospheric fine particles, studies on bacterial characterizations in submicron particles are
92 rare, especially during severe haze episodes.

93 Herein, we first characterized severe haze episodes to reveal the nutrients in submicron

94 particles from January to March 2014 in Ji'nan. The bacterial concentration and community
95 structure of different particle size fractions was analyzed subsequently. Third, we performed
96 functional analysis of the bacteria in the submicron particles to assess their potential to cause
97 risk to human health. Our study draws a framework of bacterial community in Jinan's
98 submicron particles during haze episodes and emphasizes the health risks of long-term
99 exposure to high concentrations bacteria.

100 **2. Materials and methods**

101 *2.1. Aerosol Collection.*

102 Aerosol samples were collected from the rooftop of the Lizong building in the central
103 campus of Shandong University located in Ji'nan (36°40'N, 117°3'E). The Lizong building
104 is a six-floored teaching building where classes are conducted from 08:00 to 17:00 from
105 Monday to Friday. To avoid the interference from local anthropogenic emissions on the
106 ground, a Micro-Orifice Uniform Deposit Impactor (MOUDI) and on-line monitoring
107 instruments such as SO₂ analyzer (Model 43C, Thermo, USA), NO_x analyzer (Model 42C,
108 Thermo, USA), O₃ analyzer (Model 49C, Thermo, USA) were placed in the rooftop of
109 Lizong building about 20 m from the ground. We sterilized the quartz membrane by baking
110 in a Muffle furnace at 500 °C for 6 h before sampling. After the filter cooled, it was packaged
111 into sterilized aluminum foil and stored in a sealed bag. Before sampling, the inside surfaces
112 of the MOUDI were kept sterile and 75% ethanol was used to sterilize the impactor. Seven
113 sets of aerosol samples were obtained on the 47-mm quartz membrane of the MOUDI for
114 23h (9:00 am to 8:00 am next day) at a flow rate of 30 lpm during Jan. 20, 2014 to Mar. 31,
115 2014; these samples were stored at -80 °C until analysis. Each set contained nine samples in
116 nine size-resolved ranges as follows: stage1, $\geq 18 \mu\text{m}$; stage2, 10–18 μm ; stage3, 5.6–10
117 μm ; stage4, 3.2–5.6 μm ; stage5, 1.8–3.2 μm ; stage6, 1.0–1.8 μm ; stage7, 0.56–1.0 μm ;

118 stage8, 0.32–0.56 μm ; and stage9, 0.18–0.32 μm . The $\text{PM}_{1.0}$ can easily penetrate thoracic
119 and pulmonary airways and plays an important role in haze formation and visibility
120 degradation (Shi et al., 2014). Meanwhile the fact that specific surface area of $\text{PM}_{1.0}$ is greater
121 than $\text{PM}_{2.5}$ provides evidences that $\text{PM}_{1.0}$ containing more health risks. Therefore we used
122 the stage7, stage8, and stage9 samples for the following experiments. An automatic
123 meteorological station (JZYG, PC-4) was employed to measure meteorological factors (wind
124 direction, wind speed, humidity, and temperature) in real time. Meanwhile, a Synchronized
125 Hybrid Ambient Real-Time Particulate monitor (SHARP, Model 5030, Thermo Fisher
126 Scientific, USA) and a Monitor for AeRosols and GAses analyzer (MARGA, ADI20801,
127 Applikon-ECN, Netherlands) were used to analyze the hourly average mass concentration of
128 $\text{PM}_{2.5}$, water-soluble ions, and trace gases as described previously. Based on the definition
129 of haze, seven days including six haze days (January 27, 2014; January 30, 2014; February
130 25, 2014; February 26, 2014; March 2, 2014; and March 11, 2014) and one clear day (January
131 21, 2014) were selected. Details about sampling time and the chemical characteristics
132 including $\text{PM}_{2.5}$, trace gases (SO_2 , NO_2 , and NH_3), water soluble inorganic ions (NH_4^+ , SO_4^{2-} ,
133 NH_4^+ , K^+ , Cl^- , and Na^+), and meteorological factors (wind direction and wind speed) of
134 sampling time are summarized in Figure 1.

135 2.2. DNA Extraction and PCR Amplification.

136 DNA was extracted from the quartz membrane fragments (cut into 1.1 cm^2 filter area) using
137 the E.Z.N.A.® Soil DNA Kit (Omega Bio-tek, Norcross, GA, U.S.) according to the
138 manufacturer's instructions. DNA concentration was determined using NanoDrop 2000
139 (Thermo, Wilmington, Delaware, USA). Extracted DNA samples were stored at -80°C until
140 further analysis. The V3-V4 region of 16S rRNA was amplified using a bacterial universal
141 PCR primer set 515F (5'-GTGYCAGCMGCCGCGGTAA-3') and 907R (5'-

142 CCYCAATTCMTTTRAGTTT-3') (Gallagher et al., 2013). PCR amplification was
143 performed on an ABI GeneAmp® PCR system 9700 (Applied Biosystems, 101 Foster City,
144 CA) using a 20 µL reaction mixture contained 4 µL 5×FastPfu buffer, 2 µL 2.5 mM dNTPs,
145 0.8 µL 5 µM forward primer, 0.8 µL 5 µM reverse primer, 0.4 µL Fastfu polymerase, 10 ng
146 template DNA, and 11 µL double distilled H₂O. PCR was performed at 95 °C for 3 min; 27
147 cycles of 95 °C for 10 s, 55 °C for 30 s and 72 °C for 45 s; 72 °C for 10 min; and hold at
148 10 °C. The final products were separated by 1% agarose gel electrophoresis and purified
149 using an Axygen nucleic acid purification Kit (Axygen, Biosciences, CA, USA). The purified
150 PCR products were prepared for sequencing on the Miseq™ platform (Illumina, San Diego,
151 CA, USA). The nucleotide sequences were deposited in the Sequence Read Archive (SRA)
152 under the accession number SRA385099.

153 2.3. Real-time Quantitative PCR.

154 To determine the absolute content of 16S genes in the particles of three sizes, Real-time
155 Quantitative PCR Detecting System (qPCR) was applied in this study. For the qPCR reaction
156 mixtures contained 12.5 µL of the ABI Power SybrGreen qPCR Master Mix (Promega, USA),
157 0.5 µL of each primer, 2 µL of sample DNA, and 9.5 µL of double distilled H₂O. The PCR
158 program was performed in the ABI 7500 Real-Time PCR system (Applied Biosystems, 101
159 Foster City, CA) as follows: 50 °C for 2 min; 95 °C for 15 min; 40 cycles of 95 °C for 15 s;
160 and 60 °C for 1 min. The deionized water was employed as the negative controls in this work
161 and was pipetted into the wells in a 96-well microplate with the DNA extracted from the
162 samples. All the samples were tested in triplicate and cycle thresholds worked by ABI 7500
163 software (Applied Biosystems). Based on the average rRNA gene copy number (3.98), the
164 bacterial cell concentration (cells·m⁻³) was calculated using the method described by Doorn
165 et al. (2007).

166 *2.4. High-throughput Sequence Analysis.*

167 After sequencing, the primers and barcodes were trimmed from the end of the raw sequences,
168 and low-quality reads (length less than 200 bp and average quality score less than 20) were
169 removed using FASTX-ToolKit. The sequences that passed quality control were processed
170 using QIIME (version 1.17). Alpha-diversity using the Chao1, Coverage, Simpson, and
171 Shannon indexes was also calculated at 97% similarity level. Operational taxonomic units
172 (OTU) were clustered at 97% similarity level using Uclust Soft. The ribosomal database
173 project was employed for taxonomic classification (phylum, class, order, family, and genus)
174 (Amato et al., 2013). To predict the potential functions of the bacterial communities,
175 PICRUST (Phylogenetic Investigation of Communities by Reconstruction of Unobserved
176 States, <http://picrust.github.com>) was performed using the 16S rRNA gene data. These
177 predictions were rarefied and analyzed in the Clusters of Orthologous Groups of proteins
178 (COGs) database (<http://www.ncbi.nlm.nih.gov/COG/>).

179 *2.5. Data Analysis*

180 Spearman correlation coefficients were used to visualize the relationships between bacterial
181 concentration and environmental factors (temperature, humidity, visibility, NO, NO₂, SO₂,
182 CO and O₃). The variation in bacterial abundances across three size fractions at phyla, family,
183 class, and genus level was assessed using analysis of variance (ANOVA) test. Spearman
184 correlation analysis and ANOVA test were conducted by SPSS 16.0 software (SPSS Inc.,
185 Chicago, IL). Results were considered statistically significant at P value < 0.05 and P value
186 <0.01. To describe the origin bacteria habitats, we aligned the Hiseq sequences of top 21
187 OTUs (relative abundance more than 94.5%) in NCBI database. The habitants of top five
188 highest similarities bacteria were linked to the source of airborne bacteria.

189 3. Results

190 3.1. General Characteristics of the Haze Episodes in Ji'nan.

191 The environmental factors including PM_{2.5}, water soluble inorganic ions, trace gases, wind
192 speed and wind direction were determined during sampling period. The PM_{2.5} daily average
193 mass concentration ranged from 34.3 to 422.4 $\mu\text{g}\cdot\text{m}^{-3}$ and the highest value was about 17-
194 fold higher than the daily average specified by the WHO guideline for PM_{2.5}. The mass
195 concentration of water-soluble inorganic ions and trace gases in PM_{2.5} were in the order of
196 $\text{SO}_4^{2-} > \text{NO}_3^- > \text{NH}_4^+ > \text{Cl}^- > \text{Ca}^{2+} > \text{K}^+ > \text{Mg}^{2+} > \text{Na}^+$, and $\text{SO}_2 > \text{NO}_2 > \text{NH}_3$, respectively
197 (Figure 1). The total water-soluble inorganic ions accounted for 64% of the PM_{2.5} mass
198 concentration and sulfate, nitrate, and ammonia were the most abundant compositions, which
199 were consistent with the previous report by Wang et al. (2014) who showed that SO_4^{2-} , NH_4^+
200 and NO_3^- accounted for majority of the total water-soluble ions in PM_{2.5} during the winter
201 haze in Ji'nan. Cl^- ($8.9 \mu\text{g}\cdot\text{m}^{-3}$) and K^+ ($1.5 \mu\text{g}\cdot\text{m}^{-3}$) derived from the biomass burning cannot
202 be ignored in the heating season. Du et al. (2011) determined that it was the higher
203 concentration of K^+ from the biomass burning induced pollution events. They also implied
204 that K^+ was the main existing form of KCl format in Shanghai. Meanwhile the use of
205 firecrackers and fireworks on the eve of Chinese New Year was also identified as the cause
206 for the same phenomenon (Zhang et al., 2010). The mass concentration of K^+ in the eve of
207 2014 Chinese New Year in Jinan was 18-folds higher than that in February 26, 2014. In
208 addition to these three major ions, Ca^{2+} and Mg^{2+} from continental crust sources were also
209 important during haze episodes in Ji'nan.

210 3.2. Bacterial concentration and community structure.

211 The bacterial concentration in PM_{0.18-1} was in the range of 17624-25573 $\text{cells}\cdot\text{m}^{-3}$, with an

212 average of 21509 cells·m⁻³. The maximum of bacterial concentration occurred in PM_{0.32-0.56},
213 with a value of 7314 cells·m⁻³, followed by PM_{0.18-0.32} (7212 cells·m⁻³) and PM_{0.56-1} (6982
214 cells·m⁻³) (Figure 2). After sequencing and homogenization, 27094 reads were gained for
215 each sample and a total of 236, 188, and 222 OTUs were obtained in PM_{0.18-0.32}, PM_{0.32-0.56},
216 and PM_{0.56-1}, respectively. The PM_{0.32-0.56} had the the minimum bacterial species which also
217 confirmed by the lowest Chao1 index (Table 1). The coverage of more than 99% indicates
218 the reliability of the experimental data. Meanwhile the S_{obs}/S_{Chao1} reaches 78% saturation,
219 indicating a sufficient sampling (Toti et al., 2000). In addition, PM_{0.32-0.56} and PM_{0.56-1} had
220 the same Shannon index, suggesting the similar bacterial diversity for these two particle sizes.
221 This finding was different from a previous report, where bacterial richness in fine particulate
222 matter (PM_{2.5}) was lower than that in coarse particulate matter (PM_{2.5-10}) (Bower et al., 2013).

223 In addition to bacterial concentration and alpha diversity estimators, the species comprising
224 the bacterial community also play an essential role in the evaluation of health risks. In this
225 study, 37 phyla, 71 classes, 137 orders, 236 families, and 378 genera were observed during
226 the haze episodes. The predominant bacterial phyla (relative abundance more than 1%) were
227 Firmicutes (78.9%), Proteobacteria (16.5%), Bacteroidetes (2.4%), and Actinobacteria
228 (1.7%), which corresponded to the following bacterial classes: Bacilli (78.6%),
229 Gammaproteobacteria (15.1%), Flavobacteria (2.0%), and Actinobacteria (1.7%) (Figure 3).
230 With regard to the bacteria identified at the order level, Lactobacillales, Bacillales, and
231 Pseudomonadales were found to be dominant with the relative abundances of 46.1%, 32.5%,
232 and 10.5%, respectively. At a higher taxonomic level, the most abundant genera were found
233 to be *Lactococcus*, *Bacillus*, *Pseudomonas*, and *Psychrobacter*, with relative abundances of
234 43.4%, 28.4%, 7.6%, and 2.3%, respectively (Figure 4). The dominant taxa in the bacterial
235 community in PM_{0.18-0.32}, PM_{0.32-0.56}, and PM_{0.56-1} present a similar distribution at the phyla,
236 order, and genus levels. It was consistent with those of previous studies and indicated that

237 the bacterial community structure was similar within the same seasons (Bertolini et al., 2013).
238 However, the structure of non-dominant bacteria community at different levels disclose a
239 remarkable variation (Figure 5, ANOVA, $P=0.05$, $F=2.3$). Holophagaceae (Acidobacteria)
240 were abundant in $PM_{0.32-0.56}$, displaying 6-fold times higher abundance than in $PM_{0.18-0.32}$.
241 *Acetobacter* (Proteobacteria) showed a higher relative abundance in $PM_{0.32-0.56}$, which was
242 5-fold higher than that in $PM_{0.18-0.32}$. TA06, an uncultivated candidate phylum, was found
243 only in $PM_{0.18-0.32}$. And some taxa could be found only in $PM_{0.18-0.32}$ and $PM_{0.56-1}$ such as
244 Candidate division WS3, *Rheinheimera*, and *Fastidiosipila*.

245 3.3. Implications on Human health Risks and COG Analysis.

246 Given the high diversity of inhalable bacteria, the potential influence of these bacteria on
247 humans and nature is worth noticing. 43.7% of the identified bacteria, including *Lactococcus*
248 *piscium*, *Pseudomonas fragi*, *Streptococcus agalactiae*, and *Pseudomonas cichorii*,
249 identified at the species level appeared to have interactive effects on human, animal, and
250 plant health with an average coverage of 35.4%, 7.1%, 0.7%, and 0.5%, respectively. In
251 addition to these pathogens, we also determined functional gene distribution in the airborne
252 bacterial community in this study. The COGs were considered to be related to four functional
253 groups and twenty-five function descriptions (Figure 6). Almost 80% of multi-copied genes
254 with known functions were assigned with COG codes; for example, 9.3% of the genes were
255 assigned a COG code of 'E', which represents amino acid transport and metabolism, and 7.1%
256 of the genes were found to be functionally involved in carbohydrate transport and metabolism.
257 Other codes such as K (transcription), J (translation, ribosomal structure and biogenesis), P
258 (inorganic ion transport and metabolism), M (cell wall/membrane/envelope biogenesis), and
259 C (energy production and conversion) also occupied a large proportion of the multi-copied
260 genes (more than 5%). In addition, some of the genes detected in the airborne particulate

261 matter were poorly characterized with unknown function.

262 **3. Discussion**

263 Air pollution has been studied extensively by aerosol chemistry and physics. However the
264 correlation between haze episodes and bacterial community has not been fully understood.
265 The high concentration of airborne pollutants in haze episodes may provide nutrients (sulfur,
266 nitrogen, and ammonia) and thus affect the bacterial community structure in submicron
267 particles. For example, SO_4^{2-} has a distinct ability to influence the existence and growth of
268 microbes and thus affect on their relative abundance (Scherer et al., 1981). Ca^{2+} is recognized
269 to be associated with cellular processes such as the cell cycle and cell division in bacteria and
270 can affect protein stability, enzymatic activity, and signal transduction, thus controlling
271 protein functions (Michiels et al., 2002). Cl^- , employed in chemical agents, is related to water
272 disinfection processes and thus causes bacterial stress injury. The high concentration of K^+
273 and Na^+ may disturb the structure and function of bacteria and then cause the death of bacteria.
274 Previous studies have also showed that certain bacteria were related to atmospheric dynamics.
275 For example, *Pseudomonas* species were likely to be involved in atmospheric processes such
276 as desulfuration and denitration (Robinson et al., 2012). *Bacillus* species could participate in
277 the nitrogen and carbon cycling in ecosystems (Ulrich et al., 2008). Therefore, under
278 conditions of severe air pollution, the increased concentrations of ambient pollutants in
279 submicron particles could be associated with the variation in bacterial concentration and
280 community structure.

281 In the present study, the bacterial concentration in submicron particles were much higher
282 than the China Scientific Ecology Center guideline ($1000 \text{ cells}\cdot\text{m}^{-3}$) and those reported in
283 other haze studies in China (Beijing: $224 \pm 186 \text{ CFU}\cdot\text{m}^{-3}$, and Xi'an: 1102–1736 $\text{CFU}\cdot\text{m}^{-3}$)
284 (Gao et al., 2015a; Li et al., 2015), but slightly lower or similar to those reported in some

285 previous studies in other countries (Italy: 4.6×10^5 ribosomal operons per cubic meter, about
286 1.19×10^5 cells·m⁻³, and USA: 2.72×10^4 cells·m⁻³) (Bertolini et al., 2013; Bowers et al.,
287 2012). The difference was possibly because most of the previous studies on airborne bacterial
288 concentrations were performed by the culture method, while the qPCR method was used in
289 this study. The culture method aims at the cultured bacteria which occupied only 1% of the
290 total bacteria, e.g. Gao et al. (2016) calculated the bacterial concentration
291 (705 ± 474 CFU m⁻³) during summer based on the count method. It is therefore not surprising
292 to find that the bacterial concentration reported here was much higher than that reported in
293 the other studies. This high concentration indicated that the residents in Ji'nan face higher
294 health risks. The size distribution of these airborne bacteria in submicron particles were
295 similar to the trend observed in coarse particles that Dong et al. reported, with two peaks at
296 1.1–2.1 μm and 4.7–7.0 μm , which occupied 18.6% and 19.2% of the total airborne microbes
297 collected from October 2013 to August 2014 in Qingdao (Dong et al.,2015). Dong et al.
298 (2015) believed that 71.5% of the microbes existed in the coarse particles ($>2.1 \mu\text{m}$) and
299 confirmed a distinct unimodal distribution with one peak at 2.1–3.2 μm during the heating
300 period in winter, which may be caused by a combined effect of coal combustion, higher PM,
301 and dust from the ground. Undoubtedly, in this study, all the samples were collected during
302 the heating seasons in Ji'nan; therefore, we hypothesized that the single peak observed at
303 0.32–0.56 μm may have been due to the same reason and the additional emission caused by
304 the fireworks. However, it is not clear whether airborne bacterial concentration varied with
305 changes in environmental factors. Previous study showed that PM_{2.5} and visibility showed a
306 positive and negative correlation with airborne bacterial concentration during haze episodes
307 (Li et al., 2015; Alghamdi et al.,2014; Gao et al.,2016). Goffau et al. (2009) reported that
308 gram-positive bacteria grow faster under lower relative humidity in the atmosphere. Cao et
309 al. (2014) found that the relative abundance of microbial pathogens in PM_{2.5} increased with

310 increase of air pollution level. While in this study, no obvious correlation with visibility,
311 relative humidity and PM_{2.5} were observed. The bacterial concentration exhibited a
312 significant negative correlation with NO₂ and SO₂, and O₃ (Table 2). It is likely that SO₂,
313 NO₂, and O₃ have a toxic effect on microorganisms (Abdel Hameed et al., 2012). High
314 concentration of SO₂, NO₂, and O₃ will inhibit the growth and breeding of the bacteria.

315 Due to the limit reports on the bacterial composition in PM_{1.0}, we compared the results with
316 several other studies emphasized on the bacterial composition in PM_{2.5}, PM₁₀, and TSP. At
317 the phylum level, Cao et al. (2014) showed that Actinobacteria, Proteobacteria, Chloroflexi,
318 Firmicutes, Bacteroidetes, and Euryarchaeota were the most abundant phyla in PM_{2.5} and
319 PM₁₀ during severe haze episodes. At the order level, lower abundance of Bacillales (2.0%
320 and 3.0%) and higher Actinomycetales (80.0% and 60.0%) were reported in PM_{2.5} and PM₁₀
321 samples obtained in Milan, Italy, during winter (Franzetti et al., 2011). However, the
322 abundance of Actinomycetales in the submicron particles in Ji'nan was very low in this study
323 (less than 1%, about 0.001%). This result was also markedly different from that reported by
324 Bertolini et al. (2013) who showed that Actinobacteridae, Clostridiales, and
325 Sphingobacteriales were the major taxa in the airborne bacterial community in an urban area
326 of Northern Italy. The results may be caused by the different analysis method and sequencing
327 platform. Bertolini et al. (2013) target on the V5-V6 region based on the primer 783F-1046R
328 using the Illumina GA-IIx sequencing, while our target area were V3-V4 based on the
329 universal primer (515F-907R) by Illumina Miseq platform. The different sampling and
330 analysis method produce a difference in these two studies. At the genus level, distinct
331 different bacterial community were found compared to Wang et al. (2015b) that *Arthrobacter*
332 and *Frankia* from the phylum Actinobacteria were the dominant genus in PM_{2.5} during haze
333 episodes in Beijing. From another perspective, the abundant genera (*Lactococcus*, *Bacillus*,
334 *Arthrobacter*, *Streptococcus*, *Leuconostoc*, and *Lactobacillus*) implying that about 76.4% of

335 the bacteria were recognized to be gram-positive, which is consistent with the report of Fang
336 et al. (2007) who illustrated that 80–86% of the total airborne bacteria were gram-positive in
337 outdoor environments in Beijing. The authors stated that the reason for this was that gram-
338 positive bacteria had stronger resistance and survival ability than gram-negative bacteria
339 under adverse conditions (aerosolized chemical pollutants, strong sunlight, and lower
340 humidity). While in this study, no obvious difference was observed in the abundances of
341 most abundant genus, no matter whether gram-positive or gram-negative bacteria (Figure 4).
342 The results were consistent with previous investigation by Wei et al. (2016), in that the
343 dominant bacterial community showed no significant difference between haze and clear days
344 during Jan. 2014 in Beijing. The possible explanation was the short-time sampling (less than
345 one year). Bower et al. (2012) found that the local terrestrial source environments influence
346 is more in shifting the bacterial communities, than the atmospheric condition. In future
347 studies, the quarterly and annual sampling were essential to analyze the variation between
348 haze and non-haze days.

349 Among these identified taxa, some specific bacteria were identified to be linked to human
350 health risks. *Lactococcus piscium*, a well-known pathogen to affect salmonid fish (Williams
351 et al., 1990), *Pseudomonas fragi* is responsible for bacteriological spoilage in dairy products
352 and causes great economic losses in the dairy industry (Pereira et al., 1957). *Streptococcus*
353 *agalactiae* can result in invasive infections such as skin and skin structure infections, urinary
354 tract infections, osteomyelitis, endocarditis, and meningitis in adults (Farley et al., 2001).
355 *Pseudomonas cichorii*, which is usually isolated from the soil, shows pathogenicity in plants
356 including eggplant, lettuce, celery, and chrysanthemum crops and has important economic
357 effects (Hojo et al., 2008; Pauwelyn et al., 2010). Our results show that long-term exposure
358 to high concentrations of these ambient bacteria would pose a risk to people living in such
359 hostile environments. On the other hand, the well-known beneficial bacterium *Streptococcus*

360 *thermophiles*, which has the ability to reduce the risks of antibiotic-associated diarrhea
361 and lung cancer in mice, was also detected and showed an average abundance of 0.7%
362 (Beniwal et al., 2003). In addition, bacteria with the aforementioned functions during the
363 haze episodes may have an important role in the degradation of high concentrations of
364 pollutants. For example, some species belonging to the *Streptococcus* genus have been shown
365 to be able to degrade organic acids (Amato et al., 2007); certain strains of *Sphingomonas* can
366 degrade organic matter such as polynuclear aromatic hydrocarbons (Ye et al., 1995). *Bacillus*
367 *badius* (0.5%), a well-known alkaliphilic bacterium, can degrade organic matter such as
368 aniline and anthracene (Ahmed et al., 2012).

369 The impact of airborne bacterial communities on bio-ecosystems and human health needs to
370 be investigated in future studies using bacterial cultures and metagenomics analysis.

371 Apart from the bacterial community structure in submicron particles, the source of the
372 bacteria should be identified in order to understand the inhalable microbes further. The
373 natural biosphere provides various natural environment sources for primary biological
374 aerosol particles. Generally, the primary biological aerosol reside mainly in soil, plant, rock
375 surface, leaf surface, animal secreta, skin or hair, human activity, and ocean (Bower et al.
376 2012). The microorganisms aerosolized into atmosphere and rapidly deposited rather than
377 suspended due to the high settling velocities (Despres et al. 2011). Since unique taxa may
378 exist in specific environments, the potential source of the bacteria can be identified by
379 identification of the unique taxa. In other words, the bacteria, which are derived from a
380 specific habitat can be linked to the source in the environments. During the cold season, soil
381 was an important source for the atmospheric bacteria, which was indicated by the high
382 abundance of soil-inhabiting bacteria such as *Lactococcus*, *Bacillus*, and *Arthrobacter* during
383 this season (Bowers et al., 2011). Bacteria originating from the surfaces of leaves
384 (*Pseudomonas*) have been found to be abundant in warm temperate regions (Yashiro et al.,

385 2011). Furthermore, bacteria linked to feces have been observed such as members of
386 *Escherichia* and *Streptococcus* (DeLeon-Rodriguez et al., 2013). Nevertheless, the high
387 similarities between the bacterial genera detected in the diverse seasons and locations suggest
388 that part of the airborne bacterial community may change by the spread of bacteria by long-
389 term transport (air flow from ocean, dust events, or precipitation). Jeon et al. (2011) showed
390 that airborne bacterial concentration increased significantly and the ambient bacterial
391 community structure changed markedly during dust events in Asia. However, this did not
392 seem to be the case in this study. Our results indicated that the sources of the airborne
393 bacterial community in particulate matter may be environments such as soils, leaf surfaces,
394 and feces.

395 **4. Conclusion**

396 Bacteria, including their concentration, community characteristics, correlation with
397 environmental factors, and role in infectious process of diseases and ecological process
398 may have been underestimated. In the present study, high bacterial concentration and
399 significant negative correlation with the NO₂, SO₂, and O₃ in atmosphere were detected.
400 The diverse bacteria and pathogens in submicron particles during haze episodes was
401 observed for the first time by the high-throughput sequencing, yet no significant difference
402 for the dominant bacterial genus between haze and non-haze days were observed. The results
403 also indicate that the most abundant genera show highly similarity across three size
404 fraction, while bacteria with low abundance show a significant difference such as
405 *Acetobacter* and *Fastidiosipila*. We also acknowledge that the ambient bacteria mainly
406 originated from soils, leaf surfaces, and feces. This knowledge helps for the comprehensive
407 understanding of bacterial community biodiversity in submicron particles particularly those
408 potential pathogens during haze episodes.

409 **Conflict of Interest**

410 The authors declare no conflict of interest.

411 **Acknowledgments**

412 This work was supported by the National Natural Science Foundation of China (Nos.
413 41375126, 21190053, 21527814), Taishan Scholar Grant (ts20120552), the Ministry of
414 Science and Technology of China (2014BAC22B01), and Marie Skłodowska- Curie Actions
415 (MARSU project, H2020-MSCA-RISE-2015).

416 **References**

- 417 Abdel Hameed AA, Khoder MI, Ibrahim YH, Osman ME, Ghanem S. Study on some factors
418 affecting survivability of airborne fungi. *Sci Total Environ* 2012; 414: 696-700.
- 419 Ahmed AT, Othman MA, Sarwade VD, Kachru GR. Degradation of anthracene by
420 alkaliphilic bacteria *Bacillus pasteurii*. *Environ Pollut* 2012; 1: 97-104.
- 421 Alghamdi MA, Shamy M, Redal MA, Khoder M, Awad AH, Elserougy S. Microorganisms
422 associated particulate matter: A preliminary study. *Sci Total Environ* 2014; 479–480:
423 109-116.
- 424 Amato P, Demeer F, Melaouhi A, Fontanella S, Martin-Biesse AS, Sancelme M, Laj P, Delort
425 AM. A fate for organic acids, formaldehyde and methanol in cloud water: their
426 biotransformation by microorganisms. *Atmos Chem Phys* 2007; 7: 4159-4169.
- 427 Amato KR, Yeoman CJ, Kent A, Righini N, Carbonero F, Estrada A, Gaskins HR, Stumpf
428 RM, Yildirim S, Torralba M, Gillis M, Wilson BA, Nelson KE, White BA, Leigh SR.
429 Habitat degradation impacts black howler monkey (*Alouatta pigra*) gastrointestinal
430 microbiomes. *ISME J* 2013; 7: 1344-1353.
- 431 Bauer H, Giebl H, Hitzenberger R, Kasper-Giebl A, Reischl G, Zibuschka F, Puxbaum H.

432 Airborne bacteria as cloud condensation nuclei. *J Geophys Res* 2003; 108: 1919-1964.

433 Beniwal RS, Arena VC, Thomas L, Narla S, Imperiale TF, Chaudhry RA, Ahmad UA. A
434 randomized trial of yogurt for prevention of antibiotic-associated diarrhea. *Digest Dis*
435 *Sci* 2003; 48: 2077-2082.

436 Bertolini V, Gandolfi I, Ambrosini R, Bestetti G, Innocente E, Rampazzo G, Franzetti A.
437 Temporal variability and effect of environmental variables on airborne bacterial
438 communities in an urban area of Northern Italy. *Appl Microbiol Biot* 2013; 97: 6561-
439 6570.

440 Bowers RM, McLetchie S, Knight R, Fierer NS. Spatial variability in airborne bacterial
441 communities across land-use types and their relationship to the bacterial communities
442 of potential source environments. *ISME J* 2011; 5: 601-612.

443 Bowers RM, McCubbin IB, Hallar AG, Fierer N. Seasonal variability in airborne bacterial
444 communities at a high-elevation site. *Atmos Environ* 2012; 50: 41-49.

445 Bowers RM, Clements N, Emerson JB., Wiedinmyer C, Hannigan MP, Fierer N. Seasonal
446 variability in bacterial and fungal diversity of the near-surface atmosphere. *Environ*
447 *Sci Technol* 2013; 47: 12097-12106.

448 Cao C, Jiang WJ, Wang BY, Fang JH, Lang JD, Tian G, Jiang JK, Zhu TF. Inhalable
449 microorganisms in Beijing's PM_{2.5} and PM₁₀ pollutants during a severe smog event.
450 *Environ Sci Technol* 2014; 48: 1499-1507.

451 China Meteorological Administration. Observation and forecasting levels of haze. The State
452 Standard of the People's Republic of China QX/T 113-2010 (in Chinese), Beijing:
453 China Meteorological Press; 2010.

454 Creamean JM, Suski KJ, Rosenfeld D, Cazorla A, DeMott PJ, Sullivan RC, White AB, Ralph
455 FM, Minnis P, Comstock JM, Tomlinson JM, Prather KA. Dust and biological
456 aerosols from the Sahara and Asia influence precipitation in the Western U.S. *Science*

457 2013; 339: 1572-1578.

458 DeLeon-Rodriguez N, Lathem TL, Rodriguez-R LM, Barazesh JM, Anderson BE,
459 Beyersdorf AJ, Ziemba LD, Bergin M, Nenes A, Konstantinidis KT. Microbiome of
460 the upper troposphere: species composition and prevalence, effects of tropical storms,
461 and atmospheric implications. *P Natl Acad Sci the USA* 2013; 110: 2575-80.

462 Després VR, Huffman JA, Burrows SM, Hoose C, Safatov AS, Buryak G, Frohlich-
463 Nowoisky J, Elbert W, Andreae M, Poschl U, and Jaenicke R. Primary biological
464 aerosol particles in the atmosphere: a review. *Tellus B* 2012; 64.

465 Dong LJ, Qi JH, Shao CC, Zhong X, Gao DM., Cao WW, Gao JW, Bai R, Long GY, Chu
466 CC. Concentration and size distribution of total airborne microbes in hazy and foggy
467 weather. *Sci Total Environ* 2015; 541: 1011-1018.

468 Doorn RV, Szemes M, Bonants P, Kowalchuk GA, Salles JF, Ortenberg E. Quantitative
469 multiplex detection of plant pathogens using a novel ligation probe-based system
470 coupled with universal, high-throughput real-time PCR on OpenArrays™. *BMC*
471 *Genomics* 2007; 8: 276.

472 Du HH, Kong LD, Cheng TT, Chen JM, Du JF, Li L, Xia XG, Leng CP, Huang GH. Insights
473 into summertime haze pollution events over Shanghai based on online water-soluble
474 ionic composition of aerosols. *Atmos Environ* 2011; 45: 5131-5137.

475 Esposito V, Lucariello A, Savarese L, Cinelli MP, Ferraraccio F, Bianco A, De Luca A,
476 Mazzarella G. Morphology changes in human lung epithelial cells after exposure to
477 diesel exhaust micron sub particles (PM_{1.0}) and pollen allergens. *Environ Pollut* 2012;
478 171: 162-167.

479 Fang ZG, Ouyang ZY, Zheng H, Wang XK, Hu LF. Culturable airborne bacteria in outdoor
480 environments in Beijing, China *Microb Ecol* 2007; 54: 487-496.

481 Farley M M. Group B streptococcal disease in nonpregnant adults. *Clin Infect Dis* 2001;

482 33:556-561.

483 Franzetti A, Gandolfi I, Gaspari E, Ambrosini R, Bestetti G. Seasonal variability of bacteria
484 in fine and coarse urban air particulate matter. *Appl Microbiol Biotechnol* 2011; 90:
485 745-753.

486 Gallagher LK, Glossner AW, Landkamer LL, Figueroa LA, Mandernack KW, Munakata-
487 Marr J. The effect of coal oxidation on methane production and microbial community
488 structure in Powder River Basin coal. *Int J Coal Geol* 2013; 115: 71-78.

489 Goffau MC, Yang XM, Van Dijl JM, Harmsen HM. Bacterial pleomorphism and competition
490 in a relative humidity gradient. *Environ Microbiol* 2009; 11: 809–822.

491 Gou HG, Lu JJ, Li SM, Tong YB, Xie CB, Zheng XW. Assessment of microbial communities
492 in PM1 and PM10 of Urumqi during winter. *Environ Poll* 2016; 214: 202-210.

493 Gao M, Jia RZ, Qiu TL, Han ML, Song Y, Wang XM.. Seasonal size distribution of airborne
494 culturable bacteria and fungi and preliminary estimation of their deposition in human
495 lungs during non-haze and haze days. *Atmos Environ* 2015a; 118: 203-210.

496 Gao M, Guttikunda SK, Carmichael GR, Wang WS, Liu ZR, Stanier CO, Saide PE, Yu M.
497 Health impacts and economic losses assessment of the 2013 severe haze event in
498 Beijing area. *Sci Total Environ* 2015b; 511: 553-561.

499 Gao M, Yan X, Qiu T, Han M, Wang X. Variation of correlations between factors and
500 culturable airborne bacteria and fungi. *Atmos Environ* 2016; 128: 10-19.

501 Goudarzi G, Shirmardi M, Khodarahmi F, Hashemi-Shahraki A, Alavi N, Ankali KA, Babaei
502 AA, Soleimani Z, Marzouni MB. Particulate matter and bacteria characteristics of the
503 Middle East Dust (MED) storms over Ahvaz, Iran. *Aerobiologia* 2014; 30: 345-356.

504 Haas D, Galler H, Luxner J, Zarfel G, Buzina W, Friedl H, Marth E, Habib J, Reinthaler FF.
505 The concentrations of culturable microorganisms in relation to particulate matter in
506 urban air. *Atmos Environ* 2013; 65: 215-222.

507 Han B, Zhang R, Yang W, Bai ZP, Ma ZQ, Zhang WJ. Heavy haze episodes in Beijing during
508 January 2013: Inorganic ion chemistry and source analysis using highly time-resolved
509 measurements from an urban site. *Sci Total Environ* 2016; 544: 319-329.

510 Handley BA, Webster AJF. Some factors affecting the airborne survival of bacteria outdoors.
511 *J Appl Bacteriol* 1995; 79: 368-378.

512 Hojo H, Koyanagi M, Tanaka M, Kajihara S, Ohnishi K, Kiba A, Hikichi Y. The hrp genes
513 of *Pseudomonas cichorii* are essential for pathogenicity on eggplant but not on lettuce.
514 *Microbiology* 2008;154: 2920-2928.

515 Hospodsky D, Yamamoto N, Nazaroff WW, Miller D, Gorthala S, Peccia J. Characterizing
516 airborne fungal and bacterial concentrations and emission rates in six occupied
517 children's classrooms. *Indoor Air* 2015; 25: 641-652.

518 Husman T. Health effects of indoor-air microorganisms. *Scand. J Work Env Hea* 1996; 22:
519 5-13.

520 Jansen RC, Shi Y, Chen JM, Hu YJ, Xu C, Hong SM, Li J, Zhang M. Using hourly
521 measurements to explore the role of secondary inorganic aerosol in PM_{2.5} during
522 haze and fog in Hangzhou, China. *Adv Atmos Sci* 2014; 31: 1427.
523 doi:10.1007/s00376-014-4042-2

524 Janssen NAH, Hoek G, Simic-Lawson M, Fischer P, Bree L, Brink H, Keuken M, Atkinson,
525 RW, Anderson HR, Brunekreef B, Cassee FR. Black carbon as an additional indicator
526 of the adverse health effects of airborne particles compared with PM₁₀ and PM_{2.5}.
527 *Environ Health Persp* 2011; 119: 1691-1699.

528 Jeon EM, Kim HJ, Jung K, Kim JH, Kim MY, Kim YP, Ka J. Impact of Asian dust events on
529 airborne bacterial community assessed by molecular analyses. *Atmos Environ* 2011;
530 45: 4313-4321.

531 Kong LD, Yang YW, Zhang SQ, Zhao X, Du HH, Fu HB, Zhang SC, Cheng TT, Yang X,

532 Chen JM, Wu D, Shen JD, Hong SM, Jiao L. Observations of linear dependence
533 between sulfate and nitrate in atmospheric particles. *J Geophys Res* 2014, 119: 341-
534 361.

535 Kong S, Li XX, Li L, Yin Y, Chen K, Yuan L, Zhang YJ, Shan YP, Ji YQ. Variation of
536 polycyclic aromatic hydrocarbons in atmospheric PM_{2.5} during winter haze period
537 around 2014 Chinese Spring Festival at Nanjing: Insights of source changes, air mass
538 direction and firework particle injection. *Sci Total Environ* 2015; 520: 59-72.

539 Leng CP, Cheng TT, Chen JM, Zhang RY, Tao J, Huang GH, Zha SP, Zhang MG, Fang W, Li
540 X, Li L. Measurements of surface cloud condensation nuclei and aerosol activity in
541 downtown Shanghai. *Atmos Environ* 2013; 69: 354-361.

542 Li WJ, Zhou SZ, Wang XF, Xu Z, Yuan C, Yu YC, Zhang QZ, Wang WX. Integrated
543 evaluation of aerosols from regional brown hazes over northern China in winter:
544 Concentrations, sources, transformation, and mixing states. *J Geophys Res* 2011;
545 116(D9):1-11.

546 Li M, Zhang L. Haze in China: current and future challenges. *Environ Pollut* 2014; 189: 85-
547 86.

548 Li YP, Fu HL, Wang W, Liu J, Meng QL, Wang WK. Characteristics of bacterial and fungal
549 aerosols during the autumn haze days in Xi'an, China. *Atmos Environ* 2015; 122:
550 439-447.

551 Liu ZC, Li N, Wang N. Characterization and source identification of ambient VOCs in Jinan,
552 China. *Air Qual Atmos Hlth* 2015; 9: 1-7.

553 Michiels J, Xi CW, Verhaert J, Vanderleyden J. The functions of Ca²⁺ in bacteria: a role for
554 EF-hand proteins? *Trends Microbiol* 2002; 10: 87-93.

555 Murata K, Zhang DZ. Transport of bacterial cells toward the Pacific in Northern Hemisphere
556 westerly winds. *Atmos Environ* 2014; 87:138-145.

557 Murata K, Zhang DZ. Concentration of bacterial aerosols in response to synoptic weather
558 and land-sea breeze at a seaside site downwind of the Asian continent. *J Geophys Res*
559 2016; 121, doi:10.1002/2016JD025028.

560 Pauwelyn E, Vanhouteghem K, Cottyn B, Vos PD, Maes M, Bleyaert P, Höfte M.
561 Epidemiology of *Pseudomonas cichorii*, the cause of lettuce midrib rot. *J*
562 *Phytopathol* 2011; 159: 298–305.

563 Pereira JN, Morgan ME. Nutrition and physiology of *Pseudomonas fragi*. *J Bacteriol* 1957;74:
564 710-713.

565 Prussin II AJ, Garcia EB, Marr LC. Total virus and bacteria concentrations in indoor and
566 outdoor Air. *Environ Sci Technol Lett* 2015; 2: 84-88.

567 Robinson CV, Elkins MR, Bialkowski KM, Thornton DJ, Kertesz MA. Desulfurization of
568 mucin by *Pseudomonas aeruginosa*: influence of sulfate in the lungs of cystic fibrosis
569 patients. *J Med Microbiol* 2012; 61: 1644-1653.

570 Scherer P, Sahm H. Influence of sulphur-containing compounds on the growth of
571 *Methanosarcina barkeri* in a defined medium. *Appl Microbiol Biot* 1981; 12: 28-35.

572 Shi Y, Chen JM, Hu DW, Wang L, Yang X, Wang XM. Airborne submicron particulate (PM₁)
573 pollution in Shanghai, China: Chemical variability, formation/dissociation of
574 associated semi-volatile components and the impacts on visibility. *Sci Total Environ*
575 2014; 473: 199-206.

576 Toti DS, Coyle FA, Miller JA. A structured inventory of Appalachian grass bald and heath
577 bald spider assemblages and a test of species richness estimator performance. *J*
578 *Arachnol* 2000; 28: 329-345.

579 Ulrich A, Klimke G, Wirth S. Diversity and Activity of Cellulose-Decomposing Bacteria,
580 Isolated from a Sandy and a Loamy Soil after Long-Term Manure Application.
581 *Microb Ecol* 2008; 55: 512-522.

582 Visser S, Slowik JG, Furger M, Zotter P, Bukowiecki N, Dressler R, Flechsig U, Appel K,
583 Green D, Tremper AH, Young DE, Williams PI, Allan JD, Herndon S, Williams LR,
584 Mohr C, Xu L, Ng N, Detournay A, Barlow J, Halios CH, Fleming ZL, Baltensperger
585 U, Prevot ASH. Kerb and urban increment of highly time-resolved trace elements
586 in PM₁₀, PM_{2.5} and PM_{1.0} winter aerosol in London during ClearfLo 2012. *Atmos*
587 *Chem Phys* 2015; 14: 2367-2386.

588 Wang LT, Wei Z, Chen MZ, Zheng Y. The 2013 severe haze over the southern Hebei, China:
589 model evaluation, source apportionment, and policy implications. *Atmos Chem Phys*
590 2013; 13: 28395-28451.

591 Wang XX, Chen JM, Sun JF, Li WJ, Yang LX, Wen L, Wang WX, Wang XM, Collett Jr JL,
592 Shi Y, Zhang QZ, Hu JT, Yao L, Zhu YH, Sui X, Sun XM, Mellouki A. Severe haze
593 episodes and seriously polluted fog water in Ji'nan, China. *Sci Total Environ* 2014;
594 493: 133-137.

595 Wang LW, Wen L, Xu CH, Chen JM, Wang XF, Yang LX, Wang WX, Yang X, Sui X, Yao L,
596 Zhang QZ. HONO and its potential source particulate nitrite at an urban site in North
597 China during the cold season. *Sci Total Environ* 2015a; 538: 93-101.

598 Wang BY, Lang JD, Zhang LN, Fang JH, Cao C, Hao JM, Zhu T, Tian G, Jiang JK.
599 Characterizing Beijing's airborne bacterial communities in PM_{2.5} and PM₁ samples
600 during haze pollution episodes using 16S rRNA gene analysis method. *Huan Jing Ke*
601 *Xue in Chinese* 2015b; 36: 2727-2734.

602 Wei K, Zou ZL, Zheng YH, Li J, Shen FX, Wu CY, Wu YS, Hu M, Yao MS. Ambient
603 bioaerosol particle dynamics observed during haze and sunny days in Beijing. *Sci*
604 *Total Environ* 2016; 550:751-759.

605 Williams AM, Fryer JL, Collins MD. *Lactococcus piscium* sp. nov. a new *Lactococcus*
606 species from salmonid fish. *FEMS Microbiol Lett* 1990; 56: 109-113.

- 607 Yang L, Han LZ, Chen ZL, Zhou JB, Wang J. Growing trend of China's contribution to haze
608 research. *Scientometrics* 2015; 105: 525-535.
- 609 Yashiro E, Spear RN, McManus PS. Culture-dependent and culture-independent assessment
610 of bacteria in the apple phyllosphere. *J Appl Microbiol* 2011; 110: 1284-1296.
- 611 Ye DY, Siddiqi MA, Maccubbin AE, Kumar S, Sikka HC. Degradation of polynuclear
612 aromatic hydrocarbons by *Sphingomonas paucimobilis*. *Environ Sci Technol* 1995;
613 30: 136-142.
- 614 Zhang M, Wang XM, Chen JM, Cheng TT, Wang T, Yang X, Gong YG, Geng FH, Chen CH.
615 Physical characterization of aerosol particles during the Chinese New Year's firework
616 events. *Atmos Environ* 2010; 44: 5191-5198.
- 617 Zhang JM, Chen JM, Yang LX, Sui X, Yao L, Zheng LF, Wen L, Xu CH, Wang WX. Indoor
618 PM_{2.5} and its chemical composition during a heavy haze-fog episode at Jinan, China.
619 *Atmos Environ* 2014; 99: 641-649.

620 **Table 1.** Alpha-diversity indexes (97%) from PM_{0.18-0.32}, PM_{0.32-0.56}, and PM_{0.56-1}: Sobs
 621 (number of OTUs), ACE, Chao1, Coverage, and Shannon.

Sample	N_{sequences}	Sobs	ACE	Chao1	Coverage	Shannon
PM _{0.18-0.32}	27094	236	302	289	0.99	2.48
PM _{0.32-0.56}	27094	188	293	249	0.99	2.40
PM _{0.56-1}	27094	222	292	272	0.99	2.44

622

623 **Table 2.** Spearman's correlation coefficients between airborne pollutants and meteorological
 624 parameters with bacterial concentration in PM_{0.18-0.32}, PM_{0.32-0.56}, PM_{0.18-0.32} and PM_{0.18-1} (*P
 625 < 0.05).

Bacteria	Temperature	Humidity	Visibility	PM_{2.5}	NO	NO₂	SO₂	CO	O₃
B _{0.56-1}	0.429	-0.393	0.464	-0.571	-0.071	-0.750	-0.607	0.321	-0.643
B _{0.32-0.56}	0.071	0.071	0.464	-0.571	0.429	-0.071	-0.571	-0.214	-0.143
B _{0.18-0.32}	0.571	-0.036	0.393	-0.500	-0.214	-0.821*	-0.750	0.321	-0.786*
B _{0.18-1}	0.500	-0.143	0.536	-0.679	0.000	-0.786*	-0.821*	0.250	-0.571

626

627 **List of Figures**

628 **Figure 1** Time series of the daily average ionic concentration and meteorological
629 parameters during sampling days.

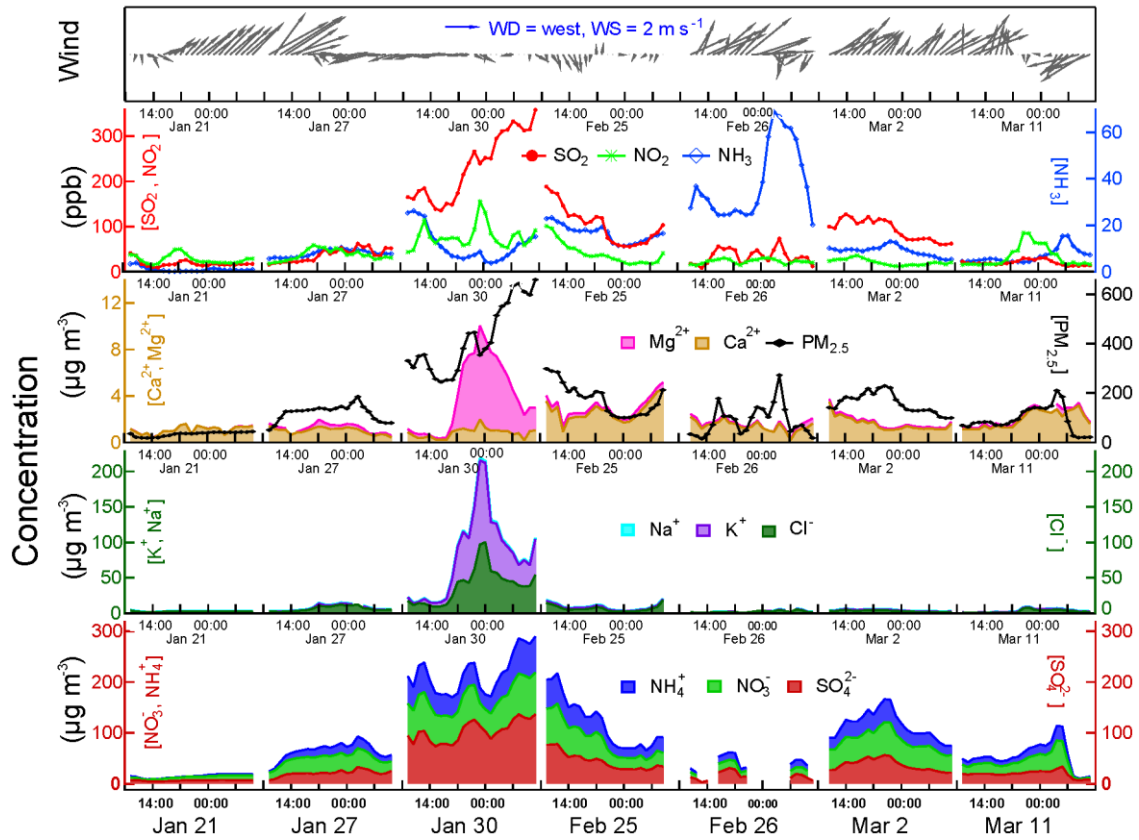
630 **Figure 2** Daily average bacterial concentration and PM mass concentration in PM_{0.56-1},
631 PM_{0.32-0.56}, and PM_{0.18-0.32}. (a-PM_{0.56-1}, b-PM_{0.32-0.56}, c-PM_{0.18-0.32}).

632 **Figure 3** (A-B) Relative abundance of bacteria at the phylum and class level in PM_{0.56-1},
633 PM_{0.32-0.56}, and PM_{0.18-0.32}. (a-PM_{0.56-1}, b-PM_{0.32-0.56}, c-PM_{0.18-0.32}).

634 **Figure 4** Heatmap of the dominant genus (relative abundance higher than 0.05%) in PM_{0.56-}
635 ₁, PM_{0.32-0.56}, and PM_{0.18-0.32} at the genus level. (a-PM_{0.56-1}, b-PM_{0.32-0.56}, c-PM_{0.18-0.32}).

636 **Figure 5** Relative abundance of the taxa (at the phyla, family, or genus levels) that were
637 found to show significant difference across aerosol size fractions: *P < 0.05, **P < 0.01.

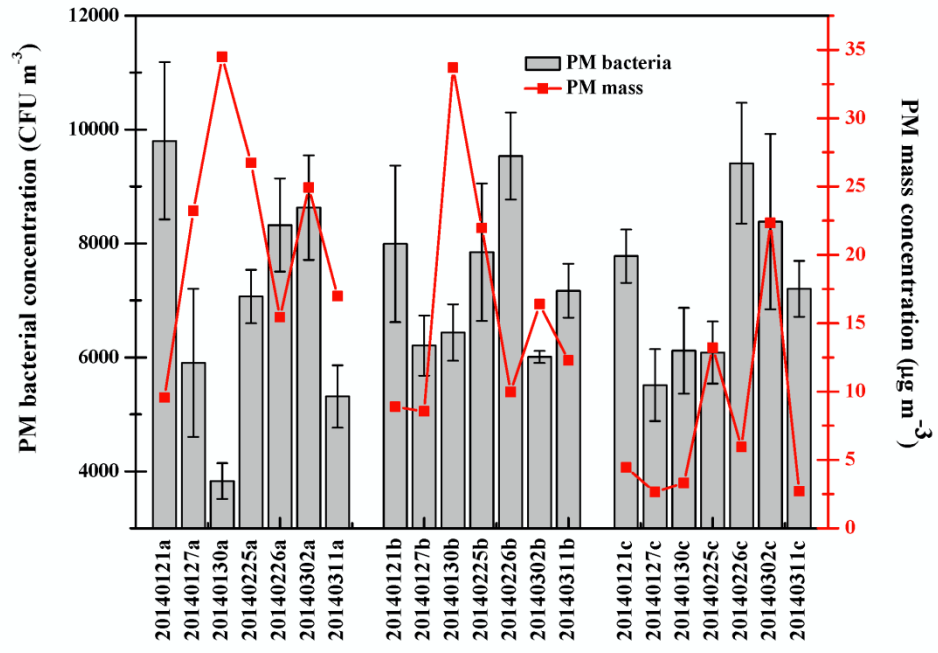
638 **Figure 6** Categorization of the microbial community genome contigs according to COGs
639 functional categories.



640

641

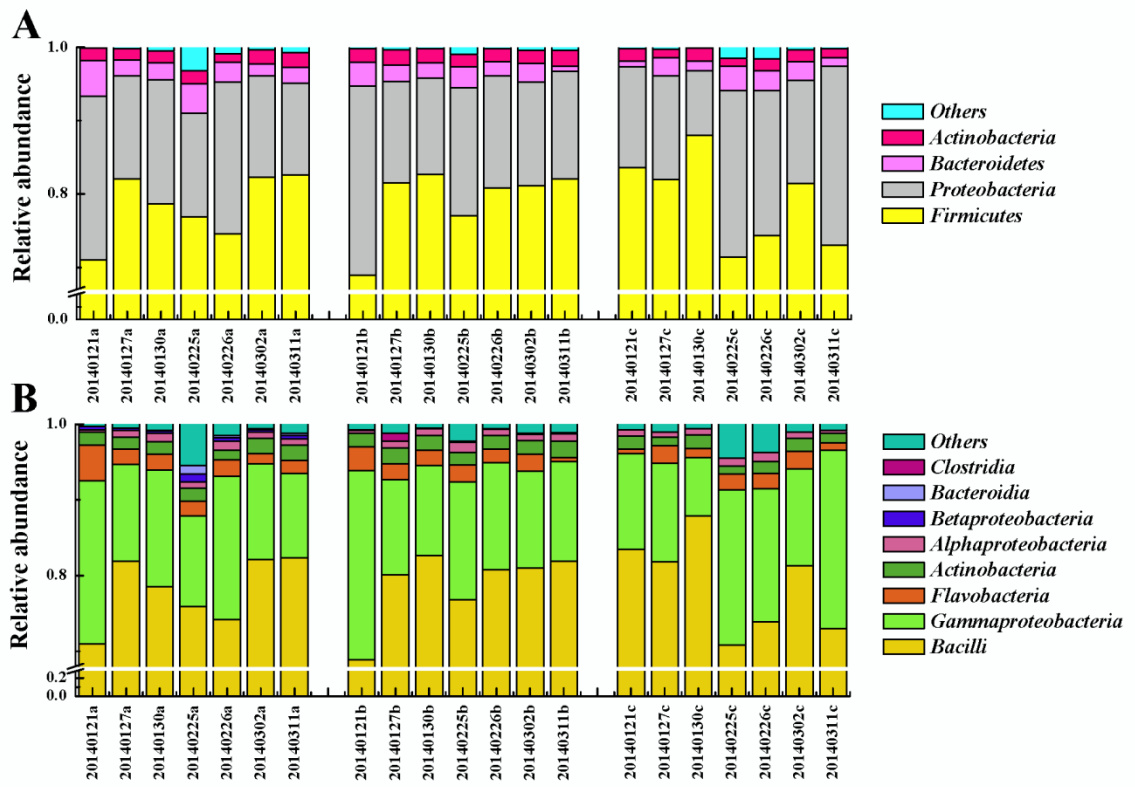
Figure 1



642

643

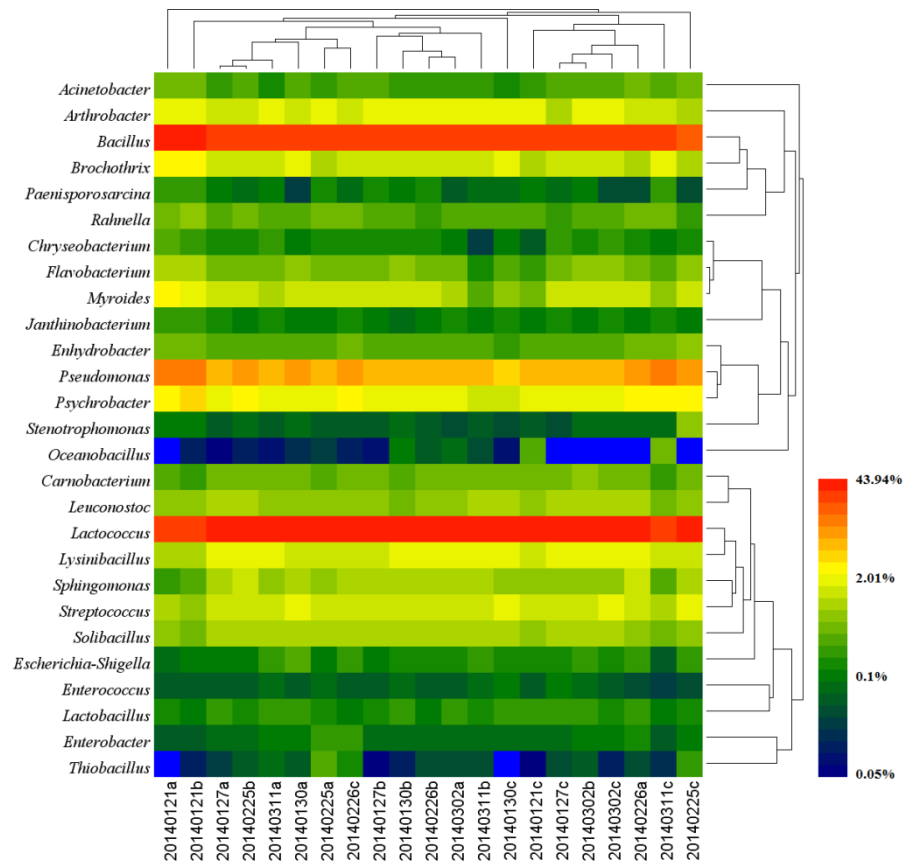
Figure 2



644

645

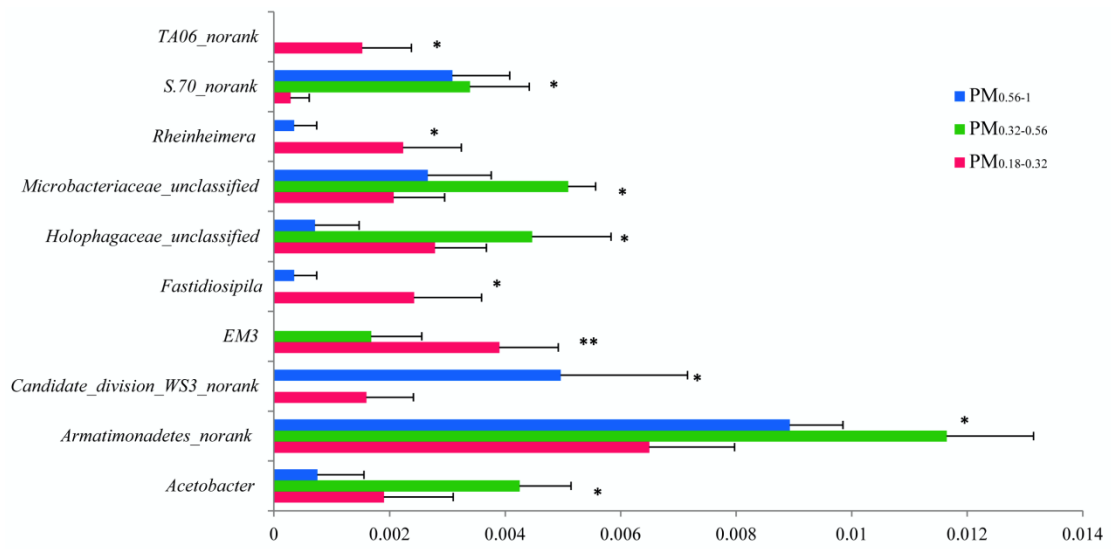
Figure 3



646

647

Figure4

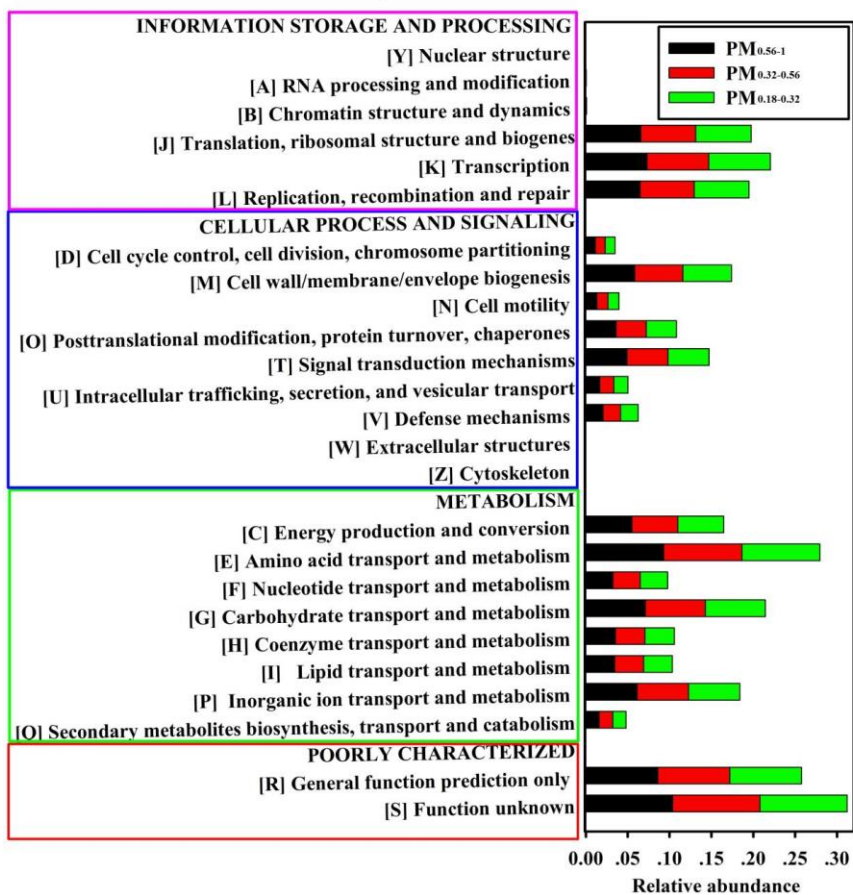


648

649

Figure 5

COG categories



650

651

Figure 6